Resonance Raman Spectroscopic Studies of Electrogenerated Cation Radicals by Column-Electrolytic Continuous-Flow Method

Munetaka Oyama, Koichi Nozaki, Hiroyuki Hatano, and Satoshi Okazaki*
Department of Chemistry, Faculty of Science, Kyoto University, Sakyo-ku, Kyoto 606
(Received June 22, 1988)

For the measurement of resonance Raman (RR) spectra of electrogenerated cation radicals in solution, a column-electrolytic continuous-flow method has been developed. This method has the advantage that the concentration of cation radicals can be easily varied by controlling the applied current. The RR spectra of the thianthrene cation radical ($TH^{+\cdot}$) have been successfully observed. The structure of $TH^{+\cdot}$ is discussed, based on the assignment of the RR band. The RR spectra of the oxidized solutions of three aromatic amines have also been measured. These spectra were assigned not due to those of cation radicals but to those of dimer cation radicals produced in the consecutive reactions.

The resonance effect in Raman spectroscopy has permitted analysis of structural and electronic changes in transient intermediates of organic compounds. These changes in many ion radicals have been studied using this technique. In most of these studies, radical anions and cations were generated by chemical and/or photochemical methods.[1-10]

In the field of electrochemistry, surface enhancement Raman scattering (SERS) and/or surface enhancement resonance Raman scattering (SERRS) have been studied extensively. A potential modulation Raman spectroscopy (PMRS) is also useful for in situ observation of electrode/electrolyte interface.[11,12] With this technique, the change in spectra of surface species with potential was obtained. In these cases, the subjects were restricted to adsorbed species on the electrode surface and/or species near electrodes. To investigate the structure of electrogenerated intermediates in dynamic state, e.g. on their chemical reactions, it is also necessary to observe their Raman spectra in bulk solution. There have been few studies, however, on electrochemically generated ion radicals in solution using resonance Raman spectroscopy (RRS).[13]

In the resonance Raman (RR) measurement of solutions by using a conventional Raman spectrophotometer with 90° scattering geometry, there are two major experimental problems as follows: (1) The concentration of a substrate must be adjusted to optimum condition.[14] (2) Decomposition and thermal absorption of the substrate by excitation laser light must be avoided. As to substrate concentration, it must be high enough to permit the RR spectrum observation. As the concentration increases, however, loss of excitation light and/or scattering light due to the absorption of a substrate also increases. So the concentration of a substrate must be adjusted carefully to the optimum range for RR measurement.

We have therefore developed a column-electrolytic continuous-flow system for Raman spectroscopy to obtain the RR spectra of electrochemically generated ion radicals in homogeneous solutions. The column electrolysis flow-cell and related techniques developed by the author (S.O.)[15,16] has been widely utilized in the preparation of organic ion radicals for their ESR,[17,18] or stopped-flow spectroscopic studies.[19,20] With this technique, it becomes easy to generate ion radicals at high concentration and vary their concentration by controlling the electrolysis current and flow rate. The second problem, decomposition and thermal absorption, can be avoided using the flow system. Thus, this method will provide the vibrational information of electrogenerated intermediates in bulk solution without any influence of the electrode conditions, such as electrode materials, pretreatments, adsorption phenomena, etc.

The present paper first describes the measurement of the resonance Raman spectra of the thianthrene (TH) cation radical ($TH^{+\cdot}$) by using this method. $TH^{+\cdot}$, one of the most stable cation radicals in acetonitrile (AN), has been the subject of a number of electrochemical studies. Recently, Jørgensen clarified its structure as being very similar to the parent molecule via ab initio MO calculation;[21] the present study also shed some light on the structure.

Also measured were the RR spectra of the oxidized AN solutions of aromatic amines such as triphenylamine (TPA), *N*-methyl-*N*-phenylaniline (MPA), and *N*,*N*-dimethylaniline (DMA). In these cases, the cation radicals of aromatic amines are unstable and dimerize rapidly. Thus we obtained the RR spectra not of monomer cation radicals but dimer cation radicals. The observed RR spectra in the flow system are discussed in connection with the absorption spectra and their consecutive reactions.

Experimental

Apparatus and Method. Visible absorption spectra were measured by a Unisoku USP-500 spectrophotometer equipped with a multichannel photodiode array detector. Raman spectra were recorded on a JEOL 400 D Raman spectrophotometer with an argon ion laser excitation source. A Toho Giken 2020 galvanostat was used for constant current electrolysis.

The outline of a column-electrolytic continuous-flow cell for Raman spectroscopy is shown in Fig. 1. The solution containing the parent molecules and supporting electrolyte

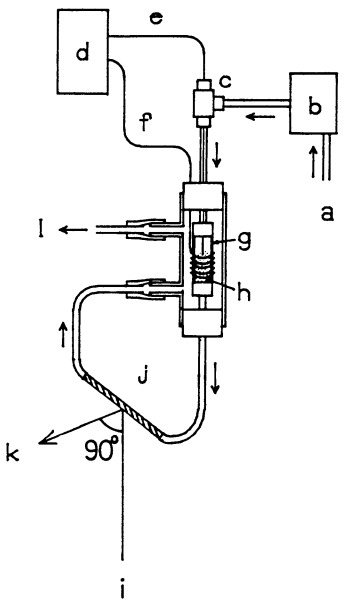

Fig. 1. Outline of the column-electrolytic continuous-flow cell for Raman spectroscopy. (a) reservoir, (b) peristaltic pump, (c) T-joint, (d) galvanostat, (e) Pt-lead to working electrode, (f) Pt-lead to counter electrode, (g) porous glass diaphragm tube, (h) carbon wool working electrode, (i) laser source, (j) capillary cell, (k) detector, (l) drain.

was sent to the column-electrolytic cell by a peristaltic pump at a constant flow rate. Acetonitrile (AN) solvent was used to acquire the RR spectra of electrogenerated cation radicals because: (1) Cation radicals are rather stable in AN. (2) AN shows relatively fewer Raman peaks than other aprotic solvents. The supporting electrolyte used was tetraethylammonium perchlorate (TEAP). The column-electrolytic cell consisted of a carbon wool working electrode which was tightly filled in a porous glass diaphragm tube (i.d. 4 mm, 3 cm length), with a platinum wire (0.3 mm) counter electrode wound outside the tube. The parent molecules were electrooxidized in the course of passing through the cell. The electrolyzed solution was then sent to a capillary cell, where the Raman spectrum was observed. The excitation light was focused from below to the capillary and the scattering light was collected at a 90° angle to the excitation light beam. The solution was then sent to the outer chamber of the cell, to serve as counter electrolyte solution and was then drained.

During measurement of a Raman spectrum, the solution flowed at a constant rate and the parent molecules were electrooxidized by constant current electrolysis. The concentration of electrogenerated cation radicals could be easily adjusted by controlling the electrolysis current and/or the sample flow rate. If the lifetime of a cation radical is sufficiently long to make the concentration decay negligible, concentration at the capillary cell can be estimated as follows:

For a simple one-electron oxidation process, the concentration of the electrogenerated cation radical, c, is given by Eq. 1,

$$c/\text{mol dm}^{-3} = \frac{\text{i/A}}{(F/\text{C mol}^{-1})\,(\text{v/dm}^3\,\text{s}^{-1})} \quad (1)$$

or Eq. 2 using practical units.

$$c/\text{mol dm}^{-3} = 6.22 \times 10^{-4}\ \frac{i/\text{mA}}{v/\text{ml min}^{-1}} \quad (2)$$

Where i, i are electrolysis current, v, v are the flow rate, and F is the Faraday constant.

Reagents. Thianthrene (Tokyo Kasei GR grade), triphenylamine, *N*-methyl-*N*-phenylaniline, and *N*,*N*-dimethylaniline (Nacalai tesque GR grade) were used without further purification. AN was twice distilled over P_2O_5. The supporting electrolyte, TEAP, was prepared by adding tetraethylammonium bromide to the aqueous solution of sodium perchlorate, recrystallizing it four times from water and drying over P_2O_5 in vacuo at 80 °C overnight before use.

The sample solutions used were 2.5 mM (1 M=1 mol dm^{-3}) TH with 0.05 M TEAP in AN and 10 mM aromatic amines with 0.1 M TEAP in AN.

Results and Discussion

Acquisition of RR Spectra of TH$^{+\cdot}$. Without the electrolysis current, the Raman spectra show only some peaks due to AN solvent, as shown in Fig. 2a, over all excitation wavelengths of the Ar^+ laser (between 457.9 and 514.5 nm). The Raman peaks of TH in AN were not observed, because (1) TH has no absorption in the region between 457.9 and 514.5 nm and (2) its concentration (2.5 mM) was too low for normal Raman measurement.

Under applied electrolysis current, by contrast, several additional Raman peaks appeared, as shown in Figs. 2b—g. These peaks were identified as the resonance Raman peaks of electrogenerated TH$^{+\cdot}$, based on

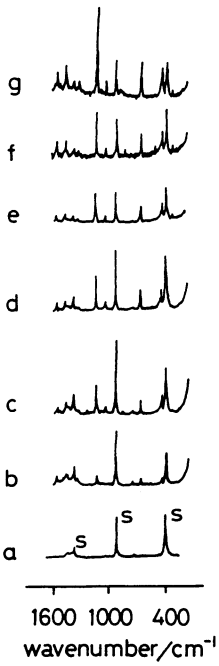

Fig. 2. Raman spectra without electrolysis current (a) and resonance Raman spectra of TH$^{+\cdot}$ (b—g) recorded between 300 and 1600 cm^{-1} using (b) 457.9, (c) 476.5, (d) 488.0, (e) 496.5, (f) 501.7, and (g) 514.5 nm excitation. Electrolysis current: 1.5 mA; flow rate: 1.1 ml min^{-1}. Solvent bands are marked with S.

the facts that (1) these peaks were observed only when the electrolysis current was applied, (2) the electrooxidized solution of TH has absorption in the Ar^+ excitation range as shown in Fig. 3; arrows indicate wavelengths of various excitation lines of the Ar^+ laser used, and (3) the absorption spectrum in Fig. 3 is in good agreement with the reported spectrum of $TH^{+\cdot}$.[22] Figures 2b—g show the effect of excitation laser wavelengths on the resonance Raman spectra of $TH^{+\cdot}$. The concentration of $TH^{+\cdot}$ was kept constant in all measurements by controlling the applied current and flow rate as the same.

Raman intensity was proportional to the excitation light intensity and the four powers of an absolute wavenumber of the peak. In the case of resonance Raman spectroscopy, excitation and scattering light were decreased by the absorption of the species. Thus, in considering the excitation profiles, we normalized the Raman peak intensities using the AN band at 920 cm^{-1}. Figure 4 shows the excitation profiles of resonance Raman peaks of $TH^{+\cdot}$. The relative intensities of all Raman bands in Fig. 4 depend on the wavelengths of the excitation laser lines and exhibit the same profile as the absorption spectrum of $TH^{+\cdot}$. This also indicates that these observed peaks are the RR peaks of $TH^{+\cdot}$.

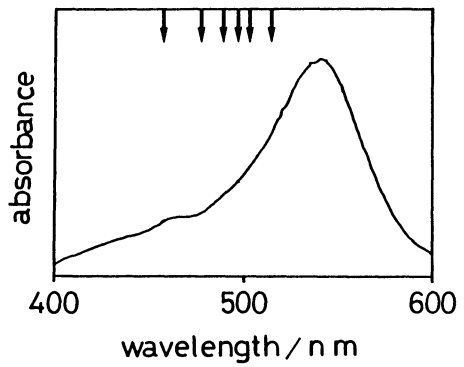

Fig. 3. Visible absorption spectrum of oxidized solution of TH. Arrows show laser lines used.

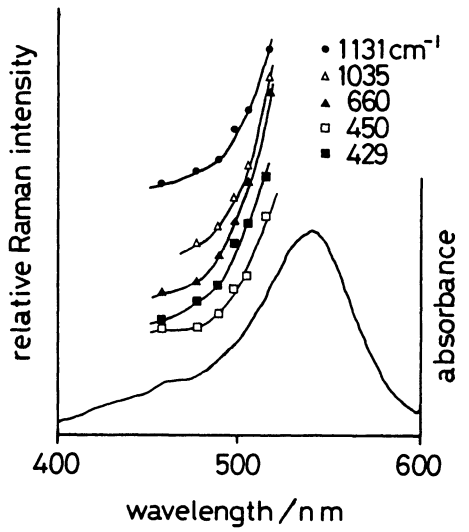

Fig. 4. Visible absorption spectrum of $TH^{+\cdot}$ and excitation profiles of resonance Raman bands, calculated using AN band at 920 cm^{-1} as internal standard.

Control of the $TH^{+\cdot}$ Concentration. Resonance Raman spectra of $TH^{+\cdot}$ were observed under various applied currents and flow rates. Table 1 summarizes the relative intensities of these $TH^{+\cdot}$ bands, normalized with the AN band at 920 cm^{-1}. The concentration of $TH^{+\cdot}$ at each run was calculated using Eq. 2. It was found that the normalized peak intensity is roughly proportional to the molar concentration of $TH^{+\cdot}$.

Figure 5 shows the effect of the electrolysis current (i.e. the concentration of $TH^{+\cdot}$) on absolute Raman intensities. In this figure, the Raman peak of AN at 381 cm^{-1} (a) and the RR peak of $TH^{+\cdot}$ at 429 cm^{-1} (b), under various applied currents at the same flow rate are shown. If there is no loss of light due to absorption by the substrate, the Raman peak of AN should have a constant intensity, while that of $TH^{+\cdot}$ should increase. The result showed, however, that the intensity of the AN band decreased and that of $TH^{+\cdot}$ band did not increase uniformly with increasing electrolysis current, owing to the absorption of the increasing $TH^{+\cdot}$. Thus, the higher concentration is not necessarily the better conditions for measurement, because the scattered light is absorbed to a great extent by the substrate itself in the 90° scattering geometry measurement.

Table 1. Relative Raman Intensities of $TH^{+\cdot}$ under Various Applied Currents and Flow Rates

Current	Flow rate	$[TH^{+\cdot}]$	Relative intensity					
			Raman sifts of $TH^{+\cdot}/cm^{-1}$					
mA	ml min^{-1}	mM	429	450	660	1035	1136	920(AN)
0.5	1.1	0.28	9	6	11	7	33	100
1.0	1.1	0.57	15	7	21	10	51	100
1.5	1.1	0.85	42	24	41	20	99	100
2.0	1.1	1.13	58	31	62	35	146	100
1.0	0.66	0.94	24	11	25	18	74	100
1.0	2.5	0.25	7	4	7	4	23	100

Excitation wavelength: 497.5 nm.

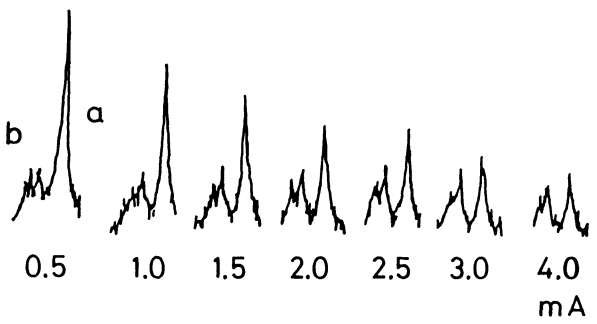

Fig. 5. Changes in intensities of AN solvent 381 cm^{-1} band (a) and $TH^{+\cdot}$ 429 cm^{-1} band (b) by applied currents. Flow rate: 1.7 ml min^{-1}; excitation wavelength: 514.5 nm.

With the electrolysis current of 4.0 mA, the RR peak of $TH^{+\cdot}$ and the Raman peak of AN became rather weak owing to the light loss due to $TH^{+\cdot}$ absorption. As a result, applied current range of 2.5 to 3.0 mA (i.e. the concentration of $TH^{+\cdot}$ was from 0.92 to 1.1 mM) was preferable for obtaining RR spectra of $TH^{+\cdot}$ with high peak intensity. Thus, it was concluded that the optimal concentration of $TH^{+\cdot}$ for the RR measurement was ca. 1.0 mM in this experiment.

Though the flow rate employed in this study was slower than 2.5 ml min^{-1} for the observation of RR spectra of very stable $TH^{+\cdot}$, faster flow-rates, up to 10 ml min^{-1}, can be applied for the acquisition of RR spectra of less short-lived species.

Comparison between the RR Spectrum of $TH^{+\cdot}$ and the Raman Spectrum of TH. The RR spectrum of $TH^{+\cdot}$ in AN (a) and the Raman spectrum of solid TH (b) are shown in Fig. 6. The Raman spectrum of TH powder was observed by the conventional procedure with a capillary cell. Vibrational modes were assigned using the reported Raman spectra of analogous molecules such as phenothiazine,[23] its cation radical,[6] and 5,10-dihydrophenazine cation radical.[8] The results are summarized in Table 2. In the case of $TH^{+\cdot}$, only nine bands were observed in this study. It seems only the most enhanced Raman bands are observed because of self-absorption.

In considering the structural difference between TH and $TH^{+\cdot}$, the significant feature is the change in its dihedral angle (θ in Fig. 7). The structure of TH has been the subject in the fields of X-ray diffraction[24] and electron diffraction.[25] It was revealed that the molecule has a folded C_{2v} conformation with a dihedral angle of 131°. Whereas, as for the structure of $TH^{+\cdot}$, it has been recently clarified by ab initio MO calculation that $TH^{+\cdot}$ is very similar in structure to TH.[21]

Hester et al. analyzed the change in dihedral angles between the phenothiazine derivatives and their cation radicals by comparing their Raman spectra.[6] In the case of phenothiazine, its dihedral angle changes in the cation radical from that of the parent molecule. This change in dihedral angle is thought to appear as the remarkable shifts in the Raman bands of the C-S-C and C-N-C skeletal deformation bands.

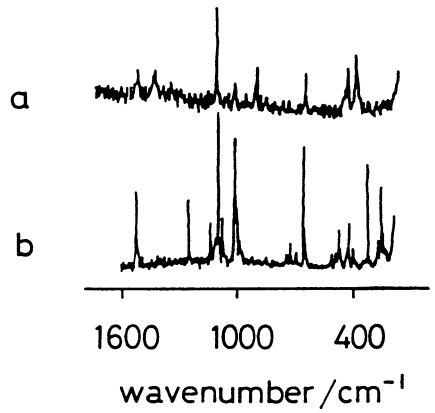

Fig. 6. Resonance Raman spectrum of $TH^{+\cdot}$ in AN (a) and Raman spectrum of solid TH (b). Excitation wavelength: 514.5 nm.

Table 2. Raman Shifts of TH and $TH^{+\cdot}$

TH[a]	$TH^{+\cdot}$[b]	Assignment
1560 s	1560 m	Ring C-C stretching
	1468 w	Riing C-C stretching
	1329 w	Riing C-C stretching
1280 s		
1160 m		
1138 w		
1118 s	1136 vs	Ring C-S-C stretching
1100 m		
1034 s	1035 m	C-H in-plane bending
1021 s		
1007 m		
	875 w	
759 w		
737 m		
704 w		
662 s	660 s	C-S stretching
516 w		
491 w		
479 m		
469 m	450 m	C-C-C in-plane skeletal deformation
428 w		
419 m	429 s	C-S-C skeletal deformation
399 w		
314 s		

Numerical data denote wavenumbers of Raman shifts (cm^{-1}). a) Solid state. b) AN solution.
Key: s=strong, v=very, m=medium, w=weak.

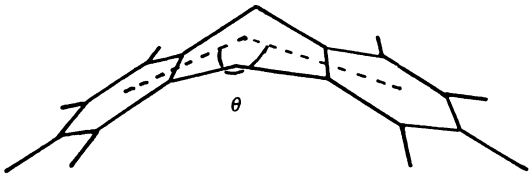

Fig. 7. Structure of $TH^{+\cdot}$. θ: dihedral angle.

In the present study, the C-S-C skeletal deformation band is assumed to correspond with the shift from 419 cm^{-1} in TH to 429 cm^{-1} in $TH^{+\cdot}$. This value is rather smaller than that of phenothiazine. It is therefore surmised that the dihedral angle of $TH^{+\cdot}$ is almost the same as that of TH, as the MO calculations predicted that the structure of $TH^{+\cdot}$ would be very similar to that of TH. However, comparison was made between TH in solid state and $TH^{+\cdot}$ in solution, since the Raman spectrum of TH could not be observed in AN owing to its poor solubility therein (10 mM). So the frequency shifts of Raman bands on dissolution of TH in AN could not be estimated. Moreover, in the short wavenumber range, the Raman spectra in the solution cannot be observed so clearly as in the solid. At present, there are still some experimental difficulties for further discussion as to the structural change in $TH^{+\cdot}$, i.e. the AN peak at 380 cm^{-1} interferes with observa-

tion of the RR spectrum of $TH^{+\cdot}$. Further investigations using other methods are needed for assessing the structural change of TH to $TH^{+\cdot}$.

RR Spectra of the Oxidized Solutions of Aromatic Amines. The RR spectra of electrooxidized solutions of the three aromatic amines TPA, MPA, and DMA were also observed by this method. Table 3 summarizes their RR shifts. For the assignment of those spectra, the reactivities of their cation radicals must be considered; that is because they dimerize rapidly and produce dimer cation radicals and/or dimer dications.

For example, on anodic oxidation of TPA, the reaction proceeds under the following schemes.[26] Here, TPB denotes *N,N,N′,N′*-tetraphenylbenzidine.

$$TPA - e^- \rightarrow TPA^{+\cdot} \quad (3)$$
$$2TPA^{+\cdot} \rightarrow TPB + 2H^+ \quad (4)$$
$$TPB - e^- \rightarrow TPB^{+\cdot} \quad (5)$$
$$TPB^{+\cdot} - e^- \rightarrow TPB^{2+} \quad (6)$$

Hinoue et al. observed in situ absorption spectra in the course of their reactions by means of internal reflection spectroscopy with an optically transparent electrode.[27]

Table 3. Raman Shifts of the Oxidized Solution of Three Aromatic Amines (a—c)[a] and $TMB^{+\cdot}$ (d)[b]

(a) TPA[a]	(b) MPA[a]	(c) DMA[a]	(d) $TMB^{+\cdot}$[b]	Assignment[b]
	1610 s		1627 w	Ring C-C str.
1579 s	1591 s	1588 vs	1602 vs	Ring C-C str.
1573 s	1560 m			
1535 m	1539 w	1555 w		
	1485 w	1489 m	1496 mw	Ring C-N str.
	1475 w	1462 w		
	1415 w	1439 w		
	1408 w	1411 m		
1324 s	1340 m	1340 m	1343 s	Inter ring C-C str.
1211 s	1241 m	1239 s	1241 s	Ring C-H i.p.b
1181 s	1224 s	1179 s	1179 m	Ring C-H i.p.b
1170 m	1129 w			
	1059 w			
994 m	995 m	989 m	991 s	Ring C-H o.p.b
935 m		941 m	941 s	Ring NX_2 wag.
901 s	879 s			
			820 m	Ring C-C str.
		808 w	807 m	Ring C-C str.
775 s	770 s	781 s	780 vvs	Ring brething
753 s	749 w	761 s	759 wm	C-H o.p.b
	660 w	634 m		
541 w				
			551 m	Ring def.
		447 w	479 m	I.p ring def.
410 w			415 m	O.p ring def.
379.w			361 w	Inter ring def.
			284 w	Inter ring def.
			252 w	Inter ring tortion
		232 m	229 m	Inter ring tortion

Numerical data denote wavenumbers of Raman shifts (cm^{-1}). a) This work. b) From Hester et al. s=strong, v=very, m=medium, w=weak, str., stretching. wag., wagging. def., deformation. i.p.b., in-plane bending. o.p.b., out of plane bending. i.p., in-plane. o.p., out of plane.

Though the absorption spectra of $TPA^{+\cdot}$ and $TPB^{+\cdot}$ could be observed, $DMA^{+\cdot}$ seemed to be so unstable and to dimerize so rapidly (within 1 ms) that the detectable species was *N,N,N′,N′*-tetramethylbenzidine (TMB) cation radical ($TMB^{+\cdot}$) or dication (TMB^{2+}).

Hester et al. obtained the RR spectrum of $TMB^{+\cdot}$ by the photoionization of TMB in a glassy ethanol matrix at 77 K (Table 3 d).[9] The obtained RR spectrum in the oxidized solution of DMA showed quite similar results in comparison with the RR spectrum of $TMB^{+\cdot}$ (Table 3 c). Furthermore, as previously reported,[28] the Raman spectrum of dimer dication differs from that of the cation radical. In the case of dianions, the Raman spectra also differed from those of anion radicals.[1] Therefore, the observed RR spectrum of the oxidized solution of DMA was assigned to $TMB^{+\cdot}$. This indicates the possibility of identifying intermediates in the course of electrochemical reactions by comparison with results from other methods.

The RR spectra of the oxidized solutions of MPA and TPA were also observed (see Table 3 a,b). In the case of MPA, the RR spectrum was assigned to *N,N′*-dimethyl-*N,N′*-diphenylbenzidine cation radical ($MPB^{+\cdot}$), considering its stability and the result of DMA. As $TPA^{+\cdot}$ is much more stable than $MPA^{+\cdot}$, $TPA^{+\cdot}$ and dimer cation radicals ($TPB^{+\cdot}$) were assumed to coexist in the capillary cell where the RR spectra were observed. The time resolved visible absorption spectra of the oxidized TPA solution were observed by column-electrolytic stopped-flow spectroscopy,[19,20] where the electrogenerated intermediate was sent rapidly to the optical flow cell and the absorption spectra at every 50 ms were observed by a multichannel photodiode array detector. The results are shown in Fig. 8, in which the decreasing peak at 651 nm was assigned to $TPA^{+\cdot}$ and the increasing peak at 464 nm was that of $TPB^{+\cdot}$. The absorption spectrum of the electrooxidized solution also indicated that $TPA^{+\cdot}$ and $TPB^{+\cdot}$ were present in the flowing solution. Though there were two species, on the basis

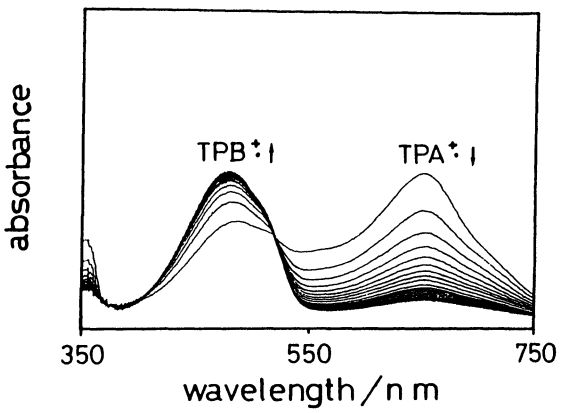

Fig. 8. Time-resolved visible absorption spectra of oxidized solution of TPA by column-electrolytic stopped-flow method.
Observation interval: 50 ms.

of the excitation wavelength (488.0 nm) the observed RR spectrum was assigned not to $TPA^{+\cdot}$ but to $TPB^{+\cdot}$. As well, the observed Raman shift of inter-ring C-C stretching band at 1324 cm^{-1} indicated that the source species is the dimer cation radical.

Though the excitation laser lines were restricted to the range between 457.9 and 514.5 nm in this study, it is very interesting that the RR spectrum of short-lived $TPA^{+\cdot}$ can be observed separately from $TPB^{+\cdot}$ using the excitation lines around 650 nm. This indicates the possibility of selective observation of the RR spectra of substances coexisting in the solution.

In conclusion, the RR spectra of electrogenerated cation radicals have been successfully measured using this method. The great feature of this method is the ease of controlling the concentration of the species, which makes the method a powerful tool for the resonance Raman study of electrogenerated intermediates in a free state, apart from electrodes.

The authors express their gratitude to Prof. Kazuhiro Maruyama for providing the Raman spectrophotometer. This work was supported in part by a Grant-in-Aid for Scientific Research, No 63470029 from the Ministry of Education, Science and Culture.

References

1) C.Takahashi and S. Maeda, *Chem. Phys. Lett.*, **22**, 364 (1973); **24**, 584 (1974); **28**, 22 (1974).
2) S. Yamaguchi, K. Yokoyama, and S. Maeda, *Bull. Chem. Soc. Jpn.*, **51**, 3193 (1978).
3) H. Kihara and Y. Gondo, *J. Raman Spectrosc.*, **17**, 263 (1986).
4) S. M. Beck and L. E. Brus, *J. Am. Chem. Soc.*, **104**, 4789 (1982).
5) G. N. P. Tripathi, D. M. Chipman, C. A. Miderski, H. Floyddavis, and R. W. Fessenden, *J. Phys. Chem.*, **90**, 3968 (1986).
6) R. E. Hester and K. P. J. Williams, *J. Chem. Soc., Parkin Trans. 2*, **1981**, 852.
7) R. E. Hester and K. P. J. Williams, *J. Chem. Soc., Parkin Trans. 2*, **1982**, 559.
8) R. E. Hester and K. P. J. Williams, *J. Raman Spectrosc.*, **13**, 91 (1982).
9) R. E. Hester and K. P. J. Williams, *J. Chem. Soc., Faraday Trans. 2*, **77**, 541 (1981).
10) R. E. Hester and K. P. J. Williams, *J. Chem. Soc., Faraday Trans. 2*, **78**, 573 (1982).
11) R. P. Van Duyne, "Chemical and Biochemical Applications of Lasers," ed by C. B. Moore, Academic Press, New York (1979), Vol. 4.
12) M. Ohsawa, K. Nisijima, and W. Suëtaka, *Surface Sci.* **104**, 270 (1981).
13) D. L. Jeanmaire and R. P. Van Duyne, *J. Am. Chem. Soc.*, **98**, 4043 (1976).
14) T. C. Strekas, D. H. Adams, A. Packer, and T. G. Spiro, *Appl. Spectrosc.*, **28**, 324 (1974).
15) S. Okazaki, *Rev. Polarogr.*, **15**, 154 (1968).
16) T. Fujinaga, T. Yamada, and S. Okazaki, *Chem. Lett.*, **1972**, 863.
17) T. Fujinaga, S. Okazaki, and T. Nagaoka, *Bull. Chem. Soc. Jpn.*, **53**, 2241 (1980).
18) T. Nagaoka, S. Okazaki, and T. Fujinaga, *J. Electroanal. Chem.*, **127**, 289 (1981).
19) M. Oyama, K. Nozaki, T. Nagaoka, H. Hatano, and S. Okazaki, *J. Chem. Soc., Perkin Trans. 2* (submitted for publication).
20) M. Oyama, K. Nozaki, H. Hatano, S. Okazaki, and T. Nagamura, 172nd meeting of the Electrochemical Soc., Honolulu, October 1987, Abstr., No. 1644.
21) K. A. Jørgensen, *Tetrahedron*, **42**, 3707 (1986).
22) E. A. C. Lucken, *J. Chem. Soc.*, **1962**, 4963.
23) B. Kure and M. D. Morris, *Talanta*, **23**, 398 (1976).
24) K. L. Gallaher and S. H. Bauer, *J. Chem. Soc., Faraday Trans. 2*, **71**, 1173 (1975).
25) I. Rowe and B. Poss, *Acta Crystallogr.*, **11**, 372 (1958).
26) E. T. Seo, R. F. Nelson, J. M. Fritsch, L. S. Marcoux, D. W. Leedy, and R. N. Adams, *J. Am. Chem. Soc.*, **88**, 3498 (1966).
27) T. Hinoue, S. Okazaki, and T. Fujinaga, *Anal. Chim. Acta*, **139**, 341 (1982).
28) D. J. Barker, R. P. Cooney, and L. A. Summer, *J. Raman Spectrosc.*, **16**, 265 (1985).